Journal Pre-proofs

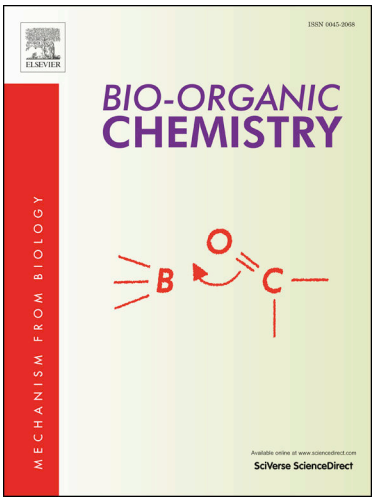

Privileged scaffold inspired design of novel oxime-biphenyl-DAPYs in treatment of HIV-1

Yang Yang, Christophe Pannecouque, Erik De Clercq, Chunlin Zhuang, Fen-Er Chen

PII: S0045-2068(20)30140-1
DOI: https://doi.org/10.1016/j.bioorg.2020.103825
Reference: YBIOO 103825

To appear in: *Bioorganic Chemistry*

Received Date: 19 January 2020
Revised Date: 11 March 2020
Accepted Date: 5 April 2020

Please cite this article as: Y. Yang, C. Pannecouque, E. De Clercq, C. Zhuang, F-E. Chen, Privileged scaffold inspired design of novel oxime-biphenyl-DAPYs in treatment of HIV-1, *Bioorganic Chemistry* (2020), doi: https://doi.org/10.1016/j.bioorg.2020.103825

Privileged scaffold inspired design of novel oxime-biphenyl-DAPYs in treatment of HIV-1

Yang Yang,[a] Christophe Pannecouque,[e] Erik De Clercq,[e] Chunlin Zhuang *[b,c] and Fen-Er Chen *[a,b,c,d]

[a.] *Sichuan Research Center for Drug Precision Industrial Technology, West China School of Pharmacy, Sichuan University, Chengdu 610041, People's Republic of China*

[b.] *Engineering Center of Catalysis and Synthesis for Chiral Molecules, Department of Chemistry, Fudan University, Shanghai 200433, People's Republic of China*

[c.] *Shanghai Engineering Center of Industrial Asymmetric Catalysis for Chiral Drugs, Shanghai 200433, People's Republic of China*

[d.] *Institute of Pharmaceutical Science and Technology, Zhejiang University of Technology Hangzhou 310014, People's Republic of China*

[e.] *Rega Institute for Medical Research, KU Leuven, Herestraat 49, B-3000 Leuven, Belgium*

** Corresponding authors. E-mail addresses: rfchen@fudan.edu.cn (F. Chen), zclnathan@163.com (C. Zhuang)*

Al

Oxime is a key pharmacophore in drug development. The biphenyl diarylpyrimidines (DAPYs) have been developed by our group as novel non-nucleoside reverse transcriptase inhibitors (NNRTIs). In this study, fourteen oxime-biphenyl-DAPYs were designed and synthesized through a privileged scaffold inspired design strategy. They exhibited promising activity toward wild type HIV-1 and single mutant strains. Compound **7d** was found to be the most potent one against both wild type (EC_{50} = 12.1 nM) and E138K mutant strains (EC_{50} = 0.0270 μM). It also had a much lower cytotoxicity (CC_{50} > 292 μM) and higher selective index (SI > 24105) than those of the FDA-approved drugs efavirenz and etravirine. Molecular docking and dynamics simulation predicted and disclosed the binding mode of compound **7d** with the RT, providing the explanation on the antiviral activity. These results were helpful for subsequent structural optimizations in anti-HIV-1 drug discovery.

Keywords: HIV-1; Oxime; Reverse transcriptase; NNRTIs; DAPY; Privileged scaffold; Molecular modelling.

Introduction

Acquired immunodeficiency syndrome (AIDS), caused by human immunodeficiency virus type 1 (HIV-1), is still a serious public health problem throughout the world [1]. Since first description of the highly active antiretroviral therapy (HAART) by Dr. Dayi He, AIDS has been effectively controlled. HAART, a regimen combining three or more kinds of antiretroviral drugs, could increase antiviral potency and reduce the development of resistance [2]. The non-nucleoside reverse transcriptase inhibitor (NNRTI) is a critical component of the HAART [3]. NNRTIs are attracting more and more focuses in the medicinal and organic chemistry communities due to its high specificity and low toxicity [4]. However, two critical issues of NNRTIs are requiring to be resolved: 1) The low solubility and poor bioavailability [3] are the main drawbacks limiting the prescription in clinic. 2) The rapid development of extensive cross-resistant strains of HIV-1 reduces the clinical efficacy of the NNRTIs.

In the last two decades, diarylpyrimidines (DAPYs) have been recognized as a series of lead compounds for structural optimization with the disclosure of etravirine (ETR) and rilpivirine (RPV) bearing a DAPY scaffold. Among them, biphenyl-DAPYs, developed by our group, were a novel series of analogues with highly potent antiviral activity against wild-type (WT) HIV-1 and a panel of clinically observed mutant strains [5-8]. Besides, the biphenyl moiety was predicted to form strong π-π stacking interactions with W229 conserved hydrophobic loop and might contribute to stabilize the conformations in the reverse transcriptase (RT) allosteric pocket [5, 7]. However, these compounds were highly hydrophobic, making the aqueous solubility still unsatisfactory [9].

Oxime, a key pharmacophore in a number of marketed drugs (Fig. 1), such as cholinesterase inhibitors, pyraloxime methiodine (2-PAM) [10], and fifth-generation cephalosporin antibiotic, ceftobiprole [11]. In addition, oxime bearing chemicals were reported to perform antiviral activities with respect to influenza virus A [12], and HIV-1 [13]. In the view of chemical structure, the oxime characterizes with both electron withdrawing group (C=N) and donating group (-O-), easily binding with

va se

interactions might be attributed to improve the biological activity as well [15].

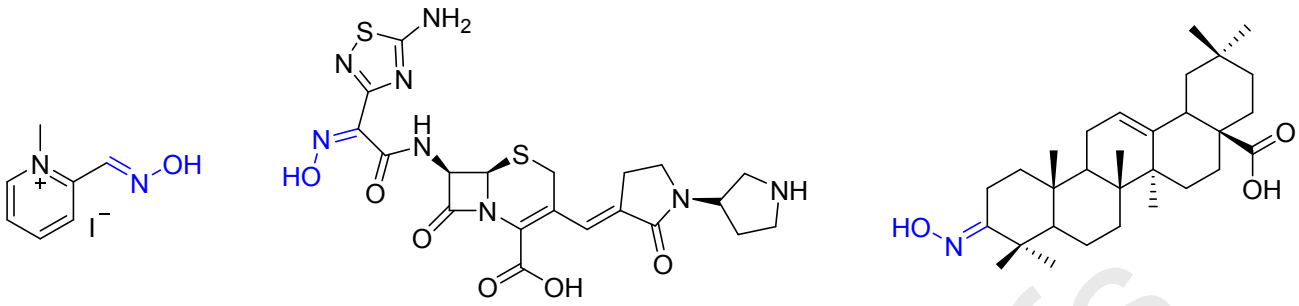

Pyraloxime Methiodide Ceftobiprole Oxime of oleanonic acid

Fig. 1 The structures of oxime-containing marketed drugs and lead compounds

Considering the strengths of the biphenyl and oxime pharmacophores, we decided to combine them into one molecule through a fusing strategy (Fig. 2). On the basis of the binding mode of the biphenyl-DAPY **1**, a water-mediated hydrogen-bonding interaction was observed at the E138 region, which should be replaced by an oxime moiety to form a similar binding interaction. The newly obtained oxime-biphenyl-DAPYs (**7a-n**) were synthesized and their structure-activity relationships (SARs) were discussed.

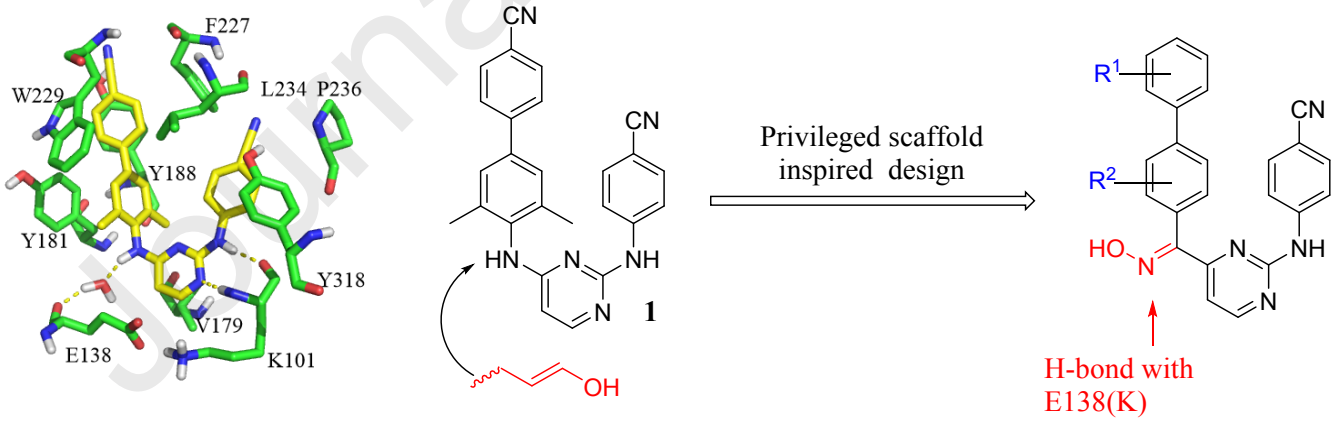

Fig. 2 The optimization strategy of biphenyl-DABPs

Results and discussion

Chemistry

The synthetic route of the target compounds is depicted in Scheme 1. Compound **4a-n** were synthesized following our established procedure (Scheme 1) [5-7]. Then, the key intermediates **6a-n** were synthesized from **5** and **4a-n** using N-heterocyclic carbene catalyzing and NaH in DMSO at room temperature under N_2 atmosphere [16, 17]. Oximation of **6a-n** with hydroxylamine sulfate in the presence of NaOH in EtOH/H_2O provided final target compounds **7a-n** [18, 19]. The final structures were characterized by ^1H NMR and ^{13}C NMR spectroscopy and HRMS.

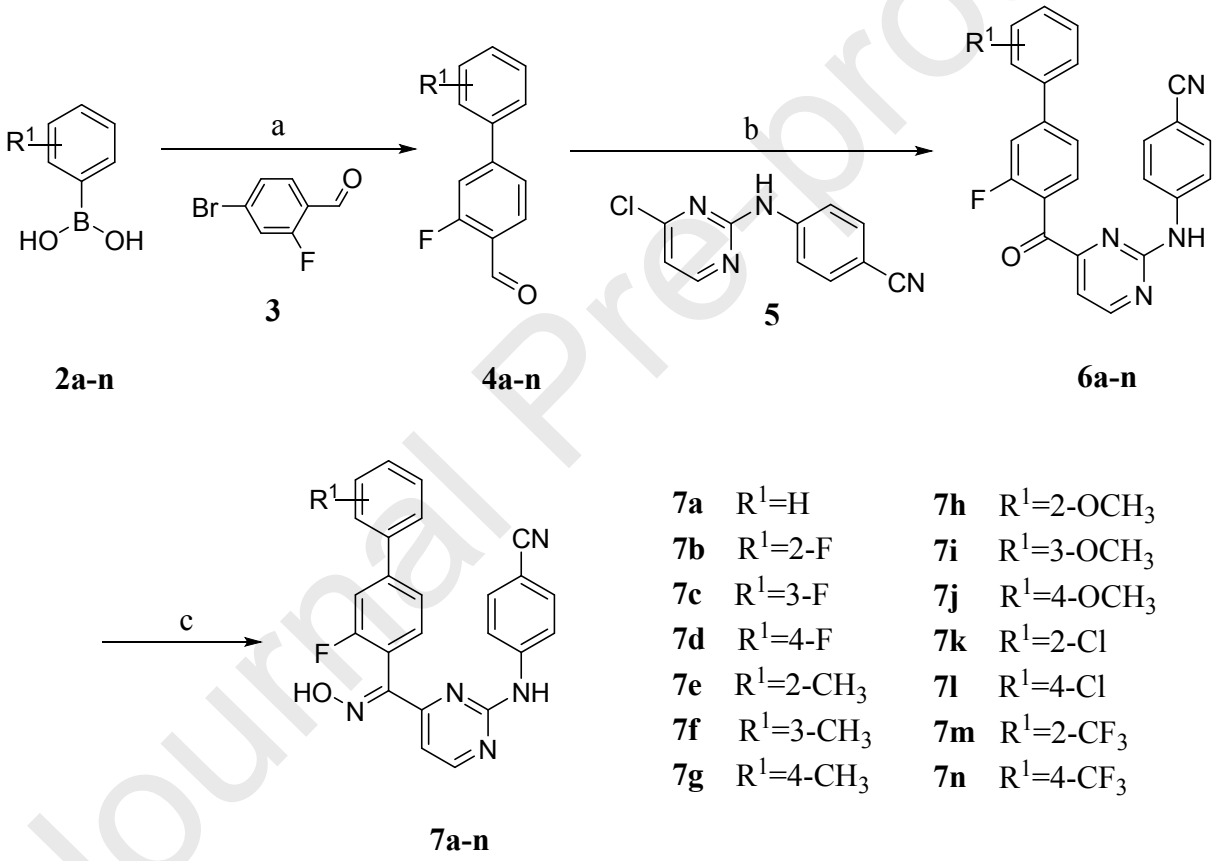

Scheme 1. Synthesis of target molecules **7a-n**.

Reagents and conditions: (a) $PdCl_2$, K_2CO_3, PEG400-H_2O, r.t., 0.5 h, N_2 protection; (b) 4-((4-chloropyrimidin-2-yl)amino)benzonitrile, NaH, 1,3-dimethyl imidazole iodide, DMSO, r.t., N_2 protection; (c) NaOH, $(NH_2OH)_2 \cdot H_2SO_4$, ethyl alcohol, 65°C.

Bi

Fourteen oxime derivatives were evaluated by the MTT method using HIV-1 infected MT-4 cells, along with nevirapine (NEV), etravirine (ETR), and efavirenz (EFV) as the reference drugs (Table 1). The inhibitory activities of the oxime derivatives against the WT HIV-1 was promising ranging from 0.0121 μM to 0.369 μM with the selectivity index (SI) ranging from 71 to 24105. Most compounds, except **7f**, **7i** and **7n,** were more potent than NVP. Compound **7a** with non-substitution on the biphenyl ring had an EC_{50} of 16.9 nM, and a CC_{50} of 29.4 μM. Fluoro-substituted analogues (**7b-d**) exhibited better activities than **7a** except **7c** with 3-F. Compound **7d** with R^1 substituted by 4-F exhibited the most potent HIV-1 inhibition (EC_{50}=12.1 nM), lowest cytotoxicity (CC_{50} > 292 μM) and best SI over 24105. Compounds **7e-g** with methyl group and **7h-j** with methoxy group exhibited similar activities to **7a** with exception of the meta-substitution. Next, we further synthesized chloro and trifluoromethyl group on *ortho*- and *para*-positions of the phenyl ring to obtain compounds **7k-n**. The activity decreased compared with **7a**. SAR analysis indicated that *ortho*- and *para*-substituted R^1 showed much better activities than *meta*-substituted analogues. The substitutions with moderate electron-withdrawing effects (e.g. F, Cl) were positive with regard to the antiviral activity. The analogues substituted with electron-donating effects (e.g. CH_3, OCH_3) or high electron-withdrawing effects (e.g. CF_3) were less active.

Table 1. Activities and cytotoxicities of compounds **7a-n** against HIV-1 (III_B) strains in MT-4 cells

compounds	R^1	**EC_{50} (μM)**[a]	**CC_{50} (μM)**[b]	**SI (III_B)**[c]
7a	H	0.0169 ± 0.009	29.4 ± 5	1740
7b	2-F	0.0149 ± 0.003	32.0 ± 0.5	2152
7c	3-F	0.0448 ± 0.02	30.9 ± 0.5	690
7d	4-F	0.0121 ± 0.002	>292	>24105
7e	2-CH_3	0.0511 ± 0.02	26.1 ± 6	511
7f	3-CH_3	0.194 ± 0.08	32.2 ± 0.1	166

7g				
7h	2-OCH_3	0.0634 ± 0.02	26.3 ± 6	415
7i	3-OCH_3	0.194 ± 0.07	23.6 ± 9	121
7j	4-OCH_3	0.0340 ± 0.01	22.5 ± 11	663
7k	2-Cl	0.0387 ± 0.01	30.8 ± 2	797
7l	4-Cl	0.0237 ± 0.01	29.9 ± 4	1259
7m	2-CF_3	0.0565 ± 0.01	28.3 ± 0.8	500
7n	4-CF_3	0.369 ± 0.1	26.3 ± 3	71
NVP		0.199 ± 0.09	>15.0	>76
EFV		0.00320 ± 0.001	>6.30	>3939
ETR		0.00460 ± 0.001	>4.60	>1012
RPV		0.00140 ± 0.0001	5.40 ± 0.3	3747

[a]EC_{50}: The effective concentration required to protect MT-4 cells against virus-induced cytopathicity by 50%.

[b]CC_{50}: The cytotoxic concentration of the compound that reduced the normal uninfected MT-4 cell viability by 50%.

[c]SI: selectivity index, ratio CC_{50}/EC_{50} (WT).

As proposed that these oxime-DAPYs might exhibit interaction with E138, we first evaluated the inhibitory activity toward the E138K mutant strain (Table 2). Consistent with the activity toward WT HIV-1, they exhibited EC_{50} values of 27.0 nM to 1.08 μM and the *ortho*- and *para*-substituted analogues showed better activities than *meta*-substituted analogues. Compound **7d** had the best activity toward the E138K mutant. However, they showed submicromolar inhibitory activities toward other single mutant strains including L100I, K103N, Y181C and double mutants (F227L + V106A, K103N + Y181C).

Ta ...RT enzyme.

compound	**EC_{50} (μM)**						
s	E138K	L100I	K103N	Y181C	Y188L	F227L + V106A	RES056(= K103N +Y181C)
7a	0.0530 ± 0.02	1.08 ± 0.2	1.95 ± 0.4	0.390 ± 0.06	3.89 ± 0.6	4.78 ± 1	9.63 ± 2
7b	0.0470 ± 0.02	0.483 ± 0.02	0.673 ± 0.03	0.217 ± 0.05	3.40 ± 0.2	3.77 ± 0.1	7.14 ± 3
7c	0.144 ± 0.9	2.46 ± 0.3	3.03 ± 0.3	0.855 ± 0.2	3.87 ± 0.3	3.67 ± 0.09	4.43 ± 1
7d	0.0270 ± 0.01	0.400 ± 0.06	0.449 ± 0.08	0.182 ± 0.04	3.43 ± 0.2	4.59 ± 0.6	22.7 ± 14
7e	0.259 ± 0.1	1.58 ± 0.5	3.30 ± 0.5	0.316 ± 0.1	4.11 ± 0.6	3.41 ± 0.2	4.09 ± 0.3
7f	0.497 ± 0.08	3.77 ± 0.1	3.94 ± 0.08	3.04 ± 0.3	4.73 ± 1	4.76 ± 1	7.70 ± 2
7g	0.160 ± 0.03	2.92 ± 1	2.81 ± 0.8	1.19 ± 0.3	5.93 ± 1	7.04 ± 1	6.42 ± 1
7h	0.360 ± 0.09	2.94 ± 0.4	3.91 ± 0.7	0.766 ± 0.2	7.71 ± 0.7	7.52 ± 0.8	7.13 ± 0.9
7i	0.690 ± 0.06	5.07 ± 2	5.45 ± 3	2.71 ± 0.7	7.91 ± 1	8.20 ± 0.8	>7.01

7j	0.06	1.44 ± 0.5	1.74 ± 0.3	0.371 ± 0.1	5.16 ± 2	5.23 ± 2	4.52 ± 1
7k	0.158 ± 0.02	1.23 ± 0.2	2.24 ± 0.3	0.314 ± 0.1	4.88 ± 1	6.17 ± 1	5.04 ± 1
7l	0.0700 ± 0.02	0.746 ± 0.1	0.699 ± 0.06	0.576 ± 0.3	3.25 ± 1	3.92 ± 0.8	4.24 ± 1
7m	0.205 ± 0.02	0.888 ± 0.3	1.14 ± 0.3	0.300 ± 0.09	3.57 ± 0.4	4.30 ± 1	3.37 ± 0.08
7n	1.08 ± 0.4	3.43 ± 0.4	2.97 ± 0.2	2.48 ± 0.5	3.52 ± 0.4	5.11 ± 0.5	7.12 ± 0.6
NVP	0.199 ± 0.1	0.976 ± 0.4	4.69 ± 0.6	4.73 ± 2	≧4.62	≧4.28	>15.0
EFV	0.00510 ± 0.002	0.0348 ± 0.006	0.0824 ± 0.01	0.00570 ± 0.001	0.241 ± 0.1	0.276 ± 0.07	0.241 ± 0.06
ETR	0.00760 ± 0.004	0.00830 ± 0.002	0.00300 ± 0.001	0.0170 ± 0.003	0.0168 ± 0.006	0.0138 ± 0.005	0.0391 ± 0.009
RPV	0.00300 ± 0.001	0.00150 ± 0.001	0.00110 ± 0.0001	0.00300 ± 0.001	0.0273 ± 0.007	0.0397 ± 0.01	0.00770 ± 0.002

Enzymatic assay of the selected compounds and Molecular docking and dynamics analysis

Compounds **7b, 7d** and **7l** were chosen to test inhibitory activity against WT HIV-1 RT enzyme (Table 3). They exhibited activities from 40.6 to 42.1 nM that were better than reference drugs NVP. As a result, the oxime-biphenyl-DAPYs effected anti-HIV activity by targeting HIV RT enzyme.

Table 3. The activity of selected compounds against WT HIV-1 RT enzyme.

Co											
$^{d}IC_{50}$ (WT RT enzyme, μM)	0.0421 ± 0.002	±	0.0421 ± 0.002	±	0.0406 ± 0.005	±	0.450 ± 0.2	±	0.00800 ± 0.003	±	

$^{d}IC_{50}$: inhibitory concentration of test compound required to inhibit WT HIV-1 RT polymerase activity by 50%.

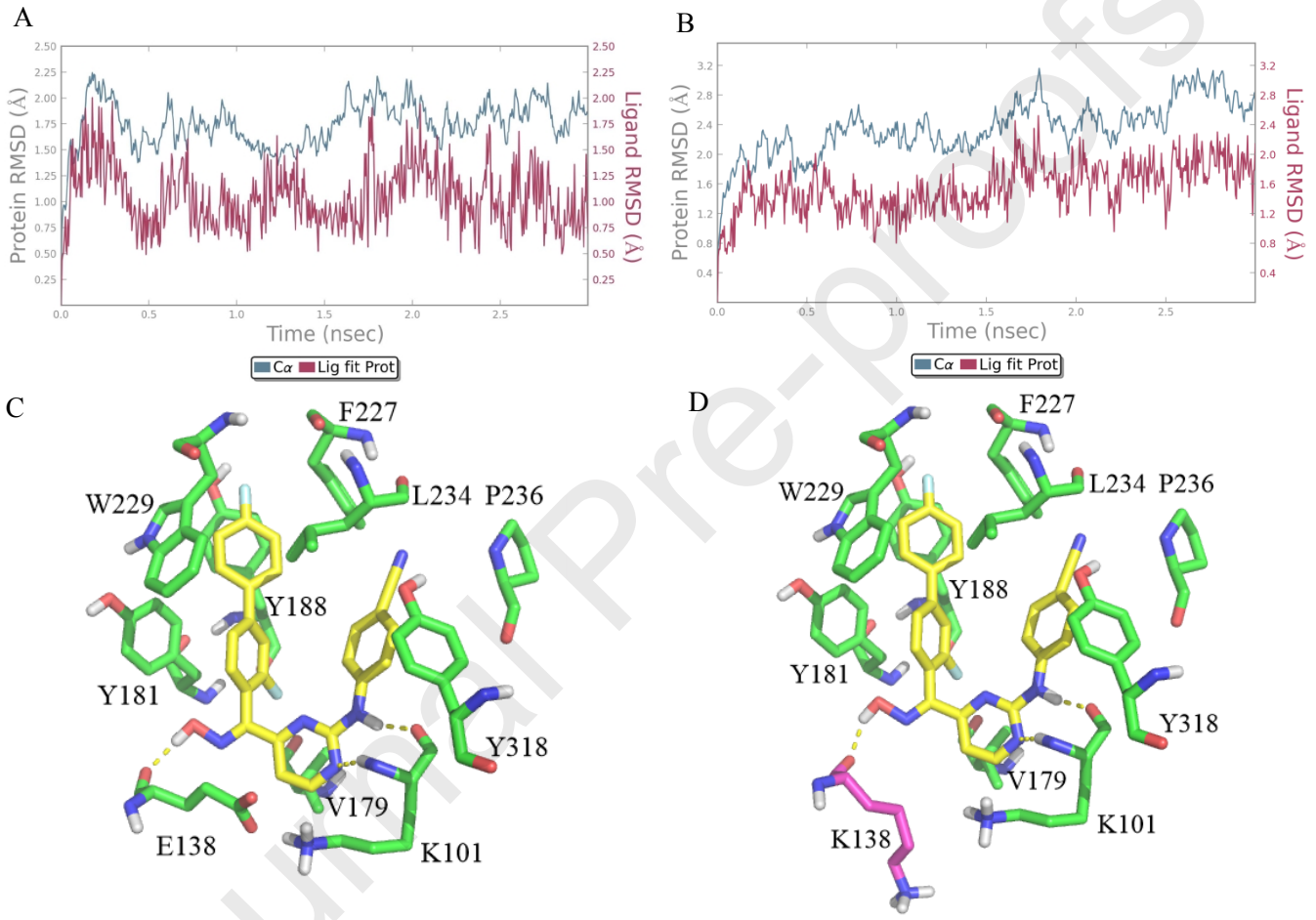

Fig. 3 Protein (PDB: 2ZD1)-Ligand (A, RT-**7d;** B, E138K-RT-**7d**) root mean square deviation (RMSD) indicates the stability of the model. Left Y-axis shows the RMSD evolution of a protein. (C) The predicted binding mode of **7d** with WT HIV-1 RT (PDB: 2ZD1). (D) The predicted binding mode of **7d** with RT (E138K). Mutated residues are depicted as pink sticks. Hydrogen bonds are depicted as yellow dashed lines.

Compound **7d** was chosen for molecular modelling study and prediction of the molecular insight after being stabilized by molecular dynamics (Fig. 3, RMSD ≈ 2 Å in 3 ns). The compound was located in the NNRTI binding pocket (NNIBP) as a typical "U" conformation [20], and formed several strong interactions with crucial amino acids of RT. The K101 residue interacted with the compound by two hydrogen bonds with the pyrimidine and the linker NH. The biphenyl fragment increased the π–π interactions with amino acid residues W229 and Y188. The newly introduced oxime, as proposed, could form a hydrogen bond with E138 (Fig. 3C) instead of the water-mediated hydrogen bond in the lead compound **1** (Fig. 2). In the E138K mutated enzyme, which was generated and minimized using BioLuminate, the compound **7d** showed very similar conformation and the hydrogen bonds with adjacent residues were maintained, especially with the K138 (Fig. 3D). The above result provided an explanation for the potency of the oxime-biphenyl-DAPYs.

As shown in Fig. 4, compound **7d** docking with NNIBP showed the common features in the other single mutant strains and double mutants, including U-shaped conformation, the hydrogen bond (K101, Fig. 4A and E138 except K103N + Y181C mutant) and hydrophobic interactions. It was worth noting that the linkage amide could form a hydrogen bond with N103 making a 10-fold higher EC_{50} than that of NVP (Fig. 4B). In the Y181C and Y188L mutants, both of the π-π interactions were reduced compared with the WT RT (Fig. 4C and Fig. 4D). In the F227L + V106A mutant, the interactions with Y181 and Y188 residues were also decreased as the mutant residues made the benzyl ring moved down or outside the hydrophobic pocket (Fig. 4E). In the K103N + Y181C mutant, the crucial hydrogen bond with E138 was lost (Fig. 4F).

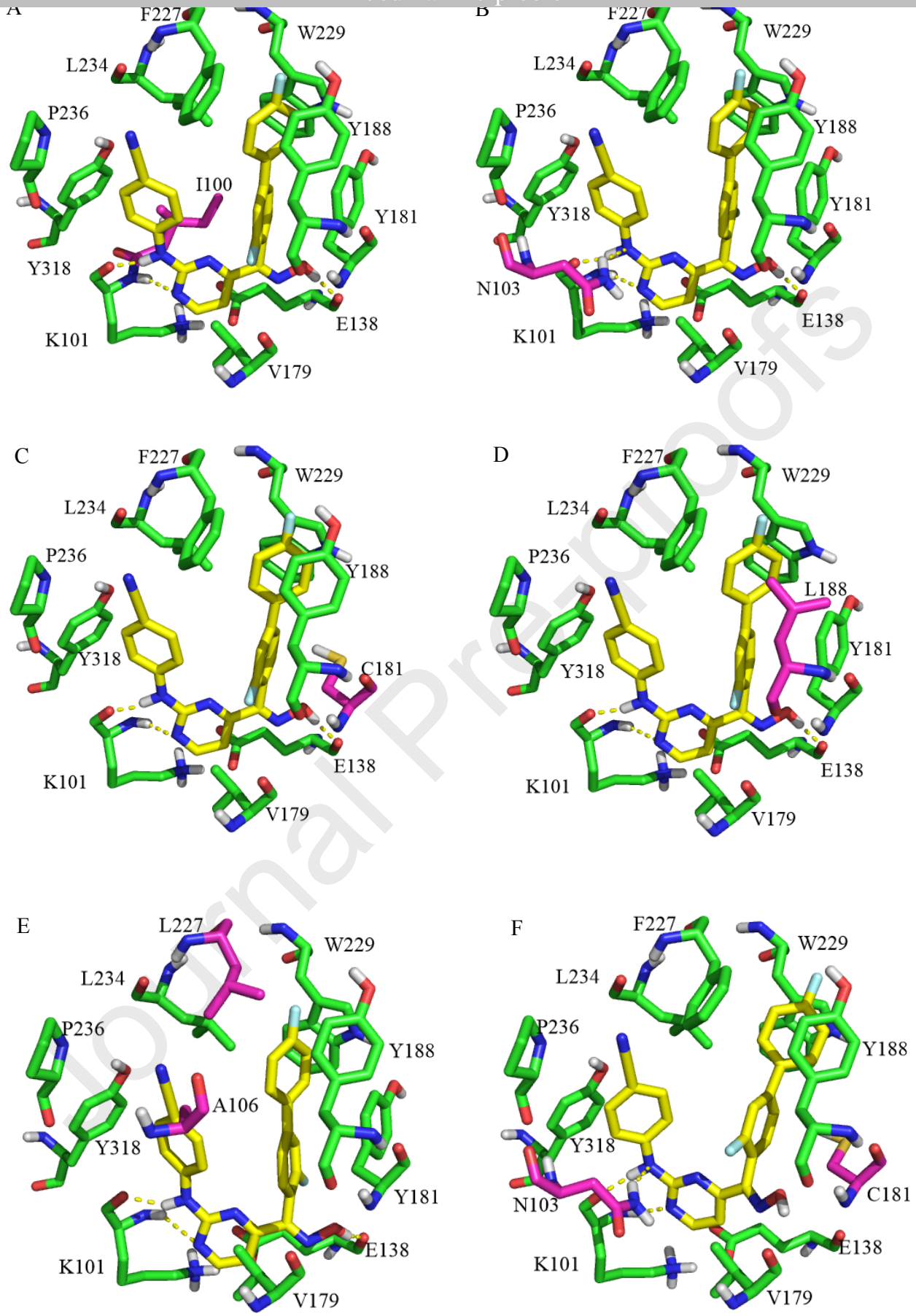

Fi (B) K103N; (C) Y181C; (D) Y188L; (E) F227L + V106A; (F) K103N + Y181C.

Conclusions

A series of oximes have been designed and synthesized by pharmacophore fusion strategy. They were demonstrated to possess nanomolar-level antiviral activity and low cytotoxicity. SAR studies led to the discovery of compound **7d** possessing 4-F, which exhibited the best antiviral activity. This compound could be fitted in the binding pocket of WT and mutants in suitable conformations and interactions. The hydrogen-bonding interactions formed by the oxime with E138 replaced the common water-mediated hydrogen bond that maintained the better activity toward WT and E138K mutant viral strains. However, the compounds exhibited much less activity toward other clinically observed single mutants and double mutants. Further optimizations based on the oxime-biphenyl-DAPYs as lead compounds are ongoing.

Experimental Procedures

Chemistry

General. All reagents and solvents were purchased from commercial sources and used without further purification. All reactions and column chromatography (silica gel of 300-400 mesh) were monitored by silica gel plates in UV light (λ = 254 nm). Melting points were measured on a WRS-1 digital melting point apparatus and are uncorrected. ^{1}H NMR spectra were recorded in DMSO-d_6 or Acetone-d_6 using a Bruker AV 400 MHz spectrometer, chemical shifts (δ) using ppm as units relative to the internal standard tetramethylsilane (TMS). HRMS were obtained on Brukersolari X-70 FT-MS instrument. The purity of the compounds **7a-n** were detected by high-performance liquid chromatography (HPLC) (Agilent 1260) using a C18 column (Eslipse XDB, 4.6*150 mm, 5 μm) with gradient methanol/water as the mobile phase at a flow rate of 0.8 mL/min: (a) 0-12 min, 50%-95% MeOH; (b) 12-20 min, 95% MeOH; (c) 20-25 min, 95%-50% MeOH; (d) 25-30 min, 50% MeOH.

General procedure for the synthesis of compounds 4a-n.

Compounds **2a-n** (1.0 mmol, 1.0 equiv.), different substituted 4-bromo-2-fluorobenzaldehyde (1.0 mmol, 1.0 equiv.), $PdCl_2$ (0.005 mmol, 0.005 equiv.) and potassium carbonate (3.5 mmol, 3.5 equiv.) were mixed in PEG400/H_2O (25 mL/25 mL) and stirred at room temperature for 30 min. The reaction was monitored by TLC. When the reactant disappearing, the reaction mixture was poured into water (80 mL) and extracted with ethyl acetate. The organic layer was washed with brine, dried over anhydrous Na_2SO_4, filtered and condensed under reduced pressure. The residue was then purified via column chromatography on silica gel, eluting with EtOAc/petroleum ether to **4a-n** as white solid.

General procedure for the synthesis of compounds 6a-n.

To a solution of **5** (1 mmol, 1.0 equiv) in anhydrous DMSO (10 mL) was added appropriate **4a-n** (1.2 mmol, 1.2 equiv) and 1,3-dimethyl imidazole iodide (0.5 mmol, 0.5 equiv). After stirred at room temperature for about 30 min, 60% NaH (2.5 mmol, 2.5 equiv) was added in portion under a nitrogen atmosphere and reacted for 4-6 h. The resulting mixture was poured into 200 mL saturated ammonium chloride solution. The precipitate was collected and purified by column chromatography, eluting with EtOAc/petroleum ether/ dichloromethane obtaining **6a-n**.

4-((4-(3-fluoro-[1,1'-biphenyl]-4-carbonyl)pyrimidin-2-yl)amino)benzonitrile (6a).

Yield: 216 mg, 55%, yellow solid, mp 180-182.3°C. ^{1}H NMR (400 MHz, DMSO-d_6) δ 10.47 (s, 1H), 8.89 (d, J = 4.9 Hz, 1H), 7.84 (t, J = 8.4 Hz, 5H), 7.78 - 7.72 (m, 2H), 7.60 (d, J = 8.4 Hz, 2H), 7.53 (t, J = 7.3 Hz, 2H), 7.47 (t, J = 7.2 Hz, 1H), 7.42 (d, J = 4.9 Hz, 1H). ^{13}C NMR (101 MHz, DMSO-d_6) δ 191.9, 162.32 (d, J_{C-F} = 94.6 Hz), 161.3, 160.3, 159.5, 147.4 (d, J_{C-F} = 8.5 Hz), 144.8, 138.1, 133.3 (2C), 132.4, 129.6 (2C), 129.5, 127.6 (2C), 124.0 (d, J_{C-F} = 13.2 Hz), 123.3, 119.8, 119.0 (2C), 114.8 (d, J_{C-F} = 22.4 Hz), 111.0, 103.4. HRMS (ESI) calcd for $[M-H]^-$ $C_{24}H_{14}FN_4O^-$: 393.1157, found: 393.1145 .

4-((4-(2',3-difluoro-[1,1'-biphenyl]-4-carbonyl)pyrimidin-2-yl)amino)benzonitrile (6b).

Yield: 255mg, 62%, yellow solid, mp 233.1-235.2°C. ^{1}H NMR (400 MHz, DMSO-d_6) δ 10.49 (s, 1H), 8.92 (d, J = 4.9 Hz, 1H), 7.93 - 7.82 (m, 3H), 7.74 - 7.58 (m, 5H), 7.58 - 7.50 (m, 1H), 7.50 - 7.32 (m, 3H). ^{13}C NMR (101 MHz, DMSO-d_6) δ 192.0, 162.4 (d, J_{C-F} = 125.3 Hz), 161.4, 159.6, 159.4 (d, J_{C-F} = 120.4 Hz), 144.8, 142.0, 133.3 (2C), 132.0, 131.5, 131.3, 125.7, 125.7, 124.7 (d, J_{C-F} = 13.7 Hz), 119.8, 119.0 (2C), 117.1, 117.0, 116.9, 116.8, 111.0, 103.4. HRMS (ESI) calcd for $[M-H]^-$ $C_{24}H_{13}F_2N_4O^-$: 411.1063, found: 411.1056.

4-((4-(3,3'-difluoro-[1,1'-biphenyl]-4-carbonyl)pyrimidin-2-yl)amino)benzonitrile (6c).

Yield: 230 mg, 56%, yellow solid, mp 218.2-219.2°C. ^{1}H NMR (400 MHz, DMSO-d_6) δ 10.45 (s, 1H), 8.89 (d, J = 4.9 Hz, 1H), 7.88 - 7.81 (m, 3H), 7.82 - 7.66 (m, 4H), 7.61 - 7.53 (m, 3H), 7.42 (d, J = 4.9 Hz, 1H), 7.33 - 7.27 (m, 1H). ^{13}C NMR (101 MHz, DMSO-d_6) δ 191.9, 163.6 (d, J_{C-F} = 171.5 Hz), 161.6, 161.3, 161.1 (d, J_{C-F} = 83.0 Hz), 159.6, 145.71 (d, J_{C-F} = 7.7 Hz), 144.8, 140.5, 133.3, 132.4 (2C), 131.6 (d, J_{C-F} = 8.4 Hz), 124.6 (d, J_{C-F} = 13.4 Hz), 123.7, 123.5, 119.8, 119.0 (2C), 116.3 (d, J_{C-F} = 20.8 Hz), 115.0 (d, J_{C-F} = 22.9 Hz), 114.5 (d, J_{C-F} = 22.9 Hz), 111.0, 103.4. HRMS (ESI) calcd for $[M+H]^+$ $C_{24}H_{15}F_2N_4O^+$: 413.1208, found: 413.1208.

4-((4-(3,4'-difluoro-[1,1'-biphenyl]-4-carbonyl)pyrimidin-2-yl)amino)benzonitrile (6d).

Yield: 268 mg, 65%, yellow solid, mp 194.1-195.6°C. ^{1}H NMR (400 MHz, DMSO-d_6) δ 10.49 (s, 1H), 8.91 (d, J = 4.8 Hz, 1H), 7.89 (ddd, J = 20.4, 8.1, 5.3 Hz, 5H), 7.77 (t, J = 11.6 Hz, 2H), 7.62 (d, J = 8.5 Hz, 2H), 7.44 (d, J = 4.8 Hz, 1H), 7.38 (t, J = 8.7 Hz, 2H). ^{13}C NMR (101 MHz, DMSO-d_6) δ 191.9, 163.6 (d, J_{C-F} = 168.9 Hz), 161.8, 161.3, 161.1 (d, J_{C-F} = 174.5 Hz), 159.5, 146.2 (d, J_{C-F} = 8.9 Hz), 144.8, 134.6, 133.4 (2C), 132.4, 129.9, 129.8, 123.9 (d, J_{C-F} = 13.3 Hz), 123.2, 119.8, 119.0 (2C), 116.7, 116.4,

11 [illegible] d: 411.1051.

4-((4-(3-fluoro-2'-methyl-[1,1'-biphenyl]-4-carbonyl)pyrimidin-2-yl)amino)benzonitrile (6e).

Yield: 232 mg, 57%, yellow solid, mp 195.6-197.0°C. ^{1}H NMR (400 MHz, DMSO-d_6) δ 10.51 (s, 1H), 8.92 (d, J = 4.9 Hz, 1H), 7.85 (dd, J = 10.6, 8.1 Hz, 3H), 7.63 (d, J = 8.8 Hz, 2H), 7.50 - 7.44 (m, 2H), 7.44 - 7.28 (m, 5H), 2.32 (s, 3H). ^{13}C NMR (101 MHz, DMSO-d_6) δ 192.1, 161.8 (d, J_{C-F} = 32.9 Hz), 161.4, 159.6, 159.4, 148.7 (d, J_{C-F} = 8.6 Hz), 144.8, 139.6, 135.3, 133.3 (2C), 131.7, 131.1, 129.8, 128.9, 126.7, 126.0, 123.8 (d, J_{C-F} = 13.3 Hz), 119.8, 119.0 (2C), 117.3 (d, J_{C-F} = 21.6 Hz), 111.1, 103.4, 20.5. HRMS (ESI) calcd for $[M+H]^+$ $C_{25}H_{18}FN_4O^+$: 409.1459, found: 409.1458.

4-((4-(3-fluoro-3'-methyl-[1,1'-biphenyl]-4-carbonyl)pyrimidin-2-yl)amino)benzonitrile (6f).

Yield: 175 mg, 43%, yellow solid, mp 195.1-197.4°C. ^{1}H NMR (400 MHz, DMSO-d_6) δ 10.48 (s, 1H), 8.91 (d, J = 4.9 Hz, 1H), 7.89 - 7.82 (m, 3H), 7.77 - 7.71 (m, 2H), 7.68 - 7.58 (m, 4H), 7.43 (dd, J = 7.9, 6.4 Hz, 2H), 7.30 (d, J = 7.5 Hz, 1H), 2.42 (s, 3H). ^{13}C NMR (101 MHz, DMSO-d_6) δ 191.9, 162.3 (d, J_{C-F} = 95.3 Hz), 161.3, 160.3, 159.6, 147.5 (d, J_{C-F} = 8.6 Hz), 144.8, 139.0, 138.1, 133.3 (2C), 132.3, 130.2, 129.6, 128.2, 124.7, 123.9 (d, J_{C-F} = 13.5 Hz), 123.3, 119.8, 119.0 (2C), 114.7 (d, J_{C-F} = 22.5 Hz), 111.0, 103.4, 21.5. HRMS (ESI) calcd for $[M+H]^+$ $C_{25}H_{18}FN_4O^+$: 409.1459, found: 409.1473.

4-((4-(3-fluoro-4'-methyl-[1,1'-biphenyl]-4-carbonyl)pyrimidin-2-yl)amino)benzonitrile (6g).

Yield: 261 mg, 64%, yellow solid, mp 215.8-216.2°C. ^{1}H NMR (400 MHz, DMSO-d_6) δ 10.47 (s, 1H), 8.91 (d, J = 4.9 Hz, 1H), 7.91 - 7.78 (m, 3H), 7.78 - 7.69 (m, 4H), 7.65 - 7.58 (m, 2H), 7.43 (d, J = 4.9 Hz, 1H), 7.35 (d, J = 8.0 Hz, 2H), 2.38 (s, 3H). ^{13}C NMR (101 MHz, DMSO-d_6) δ 191.8, 162.4 (d, J_{C-F} = 92.3 Hz), 161.2, 160.4, 159.5, 147.4 (d, J_{C-F} = 8.6 Hz), 144.9, 139.2, 135.2, 133.3 (2C), 132.4, 130.3

(2[illegible].0,

103.4, 21.2. HRMS (ESI) calcd for $[M+H]^+$ $C_{25}H_{18}FN_4O^+$: 409.1459, found: 409.1473.

4-((4-(3-fluoro-2'-methoxy-[1,1'-biphenyl]-4-carbonyl)pyrimidi-n-2-yl)amino)benzonitrile (6h).

Yield: 170 mg, 40%, yellow solid, mp 217.6-219.0°C. ^{1}H NMR (400 MHz, DMSO-d_6) δ 10.50 (s, 1H), 8.92 (d, J = 4.9 Hz, 1H), 7.87 (d, J = 8.6 Hz, 2H), 7.81 (t, J = 7.8 Hz, 1H), 7.62 (d, J = 8.6 Hz, 2H), 7.58 - 7.51 (m, 2H), 7.45 (dd, J = 6.5, 4.0 Hz, 3H), 7.22 (d, J = 8.2 Hz, 1H), 7.11 (t, J = 7.4 Hz, 1H), 3.86 (s, 3H). ^{13}C NMR (101 MHz, DMSO-d_6) δ 192.2, 161.8 (d, J_{C-F} = 15.5 Hz), 161.4, 159.6, 159.3, 156.6, 145.5, 144.9, 133.3 (2C), 131.3, 130.9, 130.8, 130.1, 126.0, 123.8 (d, J_{C-F} = 13.4 Hz), 121.5, 119.9, 119.0 (2C), 117.3 (d, J_{C-F} = 22.3 Hz), 112.5, 110.9, 103.4, 56.1. HRMS (ESI) calcd for $[M+H]^+$ $C_{25}H_{18}FN_4O_2^+$: 425.1408, found: 425.1409.

4-((4-(3-fluoro-3'-methoxy-[1,1'-biphenyl]-4-carbonyl)pyrimidi-n-2-yl)amino)benzonitrile (6i).

Yield: 148 mg, 35%, yellow solid, mp 187.3-188.7°C. ^{1}H NMR (400 MHz, DMSO-d_6) δ 10.47 (s, 1H), 8.91 (d, J = 4.9 Hz, 1H), 7.90 - 7.82 (m, 3H), 7.82 - 7.74 (m, 2H), 7.61 (d, J = 8.7 Hz, 2H), 7.46 (dd, J = 10.0, 6.2 Hz, 2H), 7.43 - 7.34 (m, 2H), 7.06 (ddd, J = 8.2, 2.6, 1.2 Hz, 1H), 3.87 (s, 3H). ^{13}C NMR (101 MHz, DMSO-d_6) δ 191.9, 162.2 (d, J_{C-F} = 96.7 Hz), 161.3, 160.4, 160.2, 159.6, 147.2 (d, J_{C-F} = 8.7 Hz), 144.8, 139.6, 133.3 (2C), 132.3, 130.8, 124.1 (d, J_{C-F} = 13.5 Hz), 123.4, 119.9, 119.8, 119.0 (2C), 115.3, 114.9 (d, J_{C-F} = 22.6 Hz), 112.9, 111.0, 103.4, 55.8. HRMS (ESI) calcd for $[M+H]^+$ $C_{25}H_{18}FN_4O_2^+$: 425.1408, found: 425.1425.

4-((4-(3-fluoro-4'-methoxy-[1,1'-biphenyl]-4-carbonyl)pyrimidin-2-yl)amino)benzonitrile (6j).

Yield: 178 mg, 42%, yellow solid, mp 216.5-218.3°C. ^{1}H NMR (400 MHz, DMSO-d_6) δ 10.49 (s, 1H), 8.90 (d, J = 4.9 Hz, 1H), 7.93 - 7.78 (m, 5H), 7.76 - 7.68 (m, 2H), 7.63 (d, J = 8.4 Hz, 2H), 7.42 (d, J = 4.9 Hz, 1H), 7.15 - 7.05 (m, 2H), 3.84 (s, 3H). ^{13}C NMR (101 MHz, DMSO-d_6) δ 191.7, 162.6 (d, J_{C-F} =

(2C), 123.0 (d, J_{C-F} = 12.9 Hz), 122.5, 119.9, 119.0 (2C), 115.1 (2C), 113.9 (d, J_{C-F} = 22.4 Hz), 111.0, 103.4, 55.8. HRMS (ESI) calcd for $[M+H]^+$ $C_{25}H_{18}FN_4O_2^+$: 425.1408, found: 425.1404.

4-((4-(2'-chloro-3-fluoro-[1,1'-biphenyl]-4-carbonyl)pyrimidin-2-yl)amino)benzonitrile (6k).

Yield: 137 mg, 32%, yellow solid, mp 265-266.7°C. ^{1}H NMR (400 MHz, DMSO-d_6) δ 10.52 (s, 1H), 8.93 (d, J = 4.9 Hz, 1H), 7.87 (dd, J = 12.8, 8.2 Hz, 3H), 7.69 - 7.65 (m, 1H), 7.62 (d, J = 8.5 Hz, 2H), 7.59-7.50 (m, 5H), 7.48 (d, J = 4.9 Hz, 1H). ^{13}C NMR (101 MHz, DMSO-d_6) δ 192.1, 161.5 (d, J_{C-F} = 35.8 Hz), 161.5, 159.6, 159.2, 145.6 (d, J_{C-F} = 8.8 Hz), 144.8, 138.1, 133.4 (2C), 131.9, 131.7, 131.6, 130.8, 130.6, 128.3, 126.3, 124.7 (d, J_{C-F} = 13.4 Hz), 119.8, 119.0 (2C), 117.7 (d, J_{C-F} = 22.5 Hz), 111.0, 103.4. HRMS (ESI) calcd for $[M+H]^+$ $C_{24}H_{15}ClFN_4O^+$: 429.0913, found: 429.0923.

4-((4-(4'-chloro-3-fluoro-[1,1'-biphenyl]-4-carbonyl)pyrimidin-2-yl)amino)benzonitrile (6l).

Yield: 141 mg, 33%, yellow solid, mp 221.3-224.1°C. ^{1}H NMR (400 MHz, DMSO-d_6) δ 10.44 (s, 1H), 8.89 (d, J = 4.9 Hz, 1H), 7.86 (td, J = 7.7, 7.1, 3.7 Hz, 5H), 7.80 - 7.72 (m, 2H), 7.59 (dd, J = 8.7, 3.7 Hz, 4H), 7.42 (d, J = 4.9 Hz, 1H). ^{13}C NMR (101 MHz, DMSO-d_6) δ 191.9, 162.2 (d, J_{C-F} = 100.7 Hz), 161.3, 160.2, 159.6, 145.9 (d, J_{C-F} = 8.7 Hz), 144.8, 136.9, 134.5, 133.3 (2C), 132.5, 129.6 (2C), 129.4 (2C), 124.3 (d, J_{C-F} = 13.3 Hz), 123.3, 119.8, 119.0 (2C), 114.8 (d, J_{C-F} = 22.8 Hz), 111.0, 103.4. HRMS (ESI) calcd for $[M+H]^+$ $C_{24}H_{15}ClFN_4O^+$: 429.0913, found: 429.0924.

4-((4-(3-fluoro-2'-(trifluoromethyl)-[1,1'-biphenyl]-4-carbonyl)pyrimidin-2-yl)amino)benzonitrile (6m).

Yield: 171 mg, 37%, yellow solid, mp 175.8-177.4°C. ^{1}H NMR (400 MHz, DMSO-d_6) δ 10.53 (s, 1H), 8.93 (d, J = 4.9 Hz, 1H), 7.92 (d, J = 7.8 Hz, 1H), 7.89 - 7.82 (m, 3H), 7.80 (d, J = 7.6 Hz, 1H), 7.72 (t, J = 7.8 Hz, 1H), 7.61 (d, J = 8.8 Hz, 2H), 7.51 (d, J = 7.6 Hz, 1H), 7.49 - 7.44 (m, 2H), 7.39 (d, J = 8.1 Hz,

1H ... J_{C-F} = 8.7 Hz), 144.8, 138.7, 133.3 (2C), 133.0, 132.2, 131.5, 129.5, 127.1 (d, J_{C-F} = 29.6 Hz), 126.8 (q, J_{C-F} = 5.3 Hz), 125.9, 124.7 (d, J_{C-F} = 13.2 Hz), 123.2, 119.8, 119.0 (2C), 117.4 (d, J_{C-F} = 22.4 Hz), 111.1, 103.4. HRMS (ESI) calcd for $[M+H]^+$ $C_{25}H_{15}F_4N_4O^+$: 463.1177, found: 463.1169.

4-((4-(3-fluoro-4'-(trifluoromethyl)-[1,1'-biphenyl]-4-carbonyl)pyrimidin-2-yl)amino)benzonitrile (6n).

Yield: 152 mg, 33%, yellow solid, mp 210.7-211.4°C. ^{1}H NMR (400 MHz, DMSO-d_6) δ 10.50 (s, 1H), 8.93 (d, J = 4.9 Hz, 1H), 8.08 (d, J = 8.0 Hz, 2H), 7.93 - 7.83 (m, 7H), 7.62 (d, J = 8.4 Hz, 2H), 7.46 (d, J = 4.8 Hz, 1H). ^{13}C NMR (101 MHz, DMSO-d_6) δ192.0, 162.1 (d, J_{C-F} = 110.8 Hz), 161.4, 160.1, 159.6, 145.5 (d, J_{C-F} = 8.3 Hz), 144.8, 142.1, 133.3 (2C), 132.5, 129.6 (d, J_{C-F} = 31.6 Hz), 128.5 (2C), 126.5 (q, J_{C-F} = 3.8 Hz), 126.0, 125.0 (d, J_{C-F} = 13.5 Hz), 123.8, 123.3, 119.8, 119.0 (2C), 115.4 (d, J_{C-F} = 23.2 Hz), 111.0, 103.4. HRMS (ESI) calcd for $[M+H]^+$ $C_{25}H_{15}F_4N_4O^+$: 463.1177, found: 463.1174.

General procedure for the synthesis of compounds 7a-n.

Compounds **6a-n** (0.5 mmol, 1.0 equiv) was solved in EtOH (25 mL) and followed by dropwise adding an aqueous solution (H_2O, 5 mL) containing NaOH (5 mmol, 10.0 equiv) and hydroxylamine sulphate (1.5 mmol, 3.0 equiv). Then, the mixture was refluxed for 1 h until complete consumption of starting material monitored by TLC. The resulting solution was poured into 100 mL ice water and neutralized with 1 N HCl. The filtrated precipitation was dried and purified by column chromatography to give compounds **7a-n**.

((4-((3-fluoro-[1,1'-biphenyl]-4-yl)(hydroxyimino)methyl)pyrim-idin-2-yl)amino)benzonitrile (7a).

Yield: 112 mg, 52%, white solid, mp 192.4-193.6°C. ^{1}H NMR (400 MHz, DMSO-d_6) δ 12.58 (s, 1H), 10.21 (s, 1H), 8.63 (d, J = 5.1 Hz, 1H), 7.83 (d, J = 7.7 Hz, 2H), 7.74 - 7.60 (m, 5H), 7.56 (t, J = 7.6 Hz,

2H[illegible].9 (d, J_{C-F} = 243.8 Hz), 159.3, 150.8, 145.1, 143.5 (d, J_{C-F} = 8.1 Hz), 139.0, 132.9 (2C), 131.9 (d, J_{C-F} = 5 Hz), 129.6 (2C), 128.8, 127.3 (2C), 122.9, 119.8, 119.6, 118.7 (2C), 114.0 (d, J_{C-F} = 22.4 Hz), 109.1, 102.7. HRMS (ESI) calcd for $[M+Na]^+$ $C_{24}H_{16}FN_5NaO^+$: 432.1231, found: 432.1219. HPLC analysis: t_R = 12.9 min; peak area, 99.7%.

((4-((2',3-difluoro-[1,1'-biphenyl]-4-yl)(hydroxyimino)methyl)pyrimidin-2-yl)amino)benzonitrile (7b).

Yield: 103 mg, 48%, white solid, mp 214.4-216.2°C. ^{1}H NMR (400 MHz, DMSO-d_6) δ 12.60 (s, 1H), 10.20 (s, 1H), 8.61 (d, J = 5.2 Hz, 1H), 7.61 (d, J = 8.5 Hz, 3H), 7.57 - 7.50 (m, 3H), 7.48 (t, J = 5.8 Hz, 3H), 7.42-7.34 (m, 5H). ^{13}C NMR (101 MHz, DMSO-d_6) δ 162.0, 159.62, 159.6 (d, J_{C-F} = 245.2 Hz), 159.3,159.3 (d, J_{C-F} = 244.2 Hz), 150.7, 145.1, 138.2 (d, J_{C-F} = 8.2 Hz), 132.9 (2C), 131.7 (d, J_{C-F} = 4.7 Hz), 131.3, 131.3, 130.9 (d, J_{C-F} = 8.6 Hz), 125.7 (d, J_{C-F} = 3.7 Hz), 125.2 (d, J_{C-F} = 17.8 Hz), 119.8, 118.7 (2C), 116.9, 116.7, 109.1, 102.7. HRMS (ESI) calcd for $[M+H]^+$ $C_{24}H_{16}F_2N_5O^+$: 428.1317, found: 428.1325. HPLC analysis: t_R = 13.1 min; peak area, 99.2%.

((4-((3,3'-difluoro-[1,1'-biphenyl]-4-yl)(hydroxyimino)methyl)pyrimidin-2-yl)amino)benzonitrile (7c).

Yield: 111 mg, 52%, white solid, mp >250°C. ^{1}H NMR (400 MHz, DMSO-d_6) δ 12.60 (s, 1H), 10.20 (s, 1H), 8.63 (d, J = 5.2 Hz, 1H), 7.76 (dd, J = 16.2, 8.6 Hz, 3H), 7.70 (d, J = 8.3 Hz, 2H), 7.63 (d, J = 8.8 Hz, 2H), 7.52 - 7.45 (m, 2H), 7.38 (d, J = 8.5 Hz, 2H), 7.34 - 7.27 (m, 1H). ^{13}C NMR (101 MHz, DMSO) δ 162.77 (d, J_{C-F} = 341.9 Hz), 162.1, 159.7 (d, J_{C-F} = 122.4 Hz), 159.6, 159.3, 150.7, 145.1, 142.0 (d, J_{C-F} = 8.1 Hz), 141.3 (d, J_{C-F} = 7.7 Hz), 132.9 (2C), 132.0 (d, J_{C-F} = 4.7 Hz), 131.6 (d, J_{C-F} = 8.7 Hz), 123.38, 122.99, 120.35 (d, J_{C-F} = 18 Hz), 119.76, 118.7 (2C), 115.6 (d, J_{C-F} = 21.2 Hz), 114.2 (d, J_{C-F} = 22.9 Hz),

11 [illegible] d: 428.1307. HPLC analysis: t_R = 13.2 min; peak area, 98.9%.

4-((4-((2',3-difluoro-[1,1'-biphenyl]-4-yl)(hydroxyimino)methyl)pyrimidin-2-yl)amino)benzonitrile (7d).

Yield: 124 mg, 58%, white solid, mp: 204.4-206.4°C. ^{1}H NMR (400 MHz, DMSO-d_6) δ 12.56 (s, 1H), 10.18 (s, 1H), 8.63 (d, J = 5.2 Hz, 1H), 7.93 - 7.84 (m, 2H), 7.74 - 7.60 (m, 4H), 7.46 (dd, J = 9.2, 6.3 Hz, 2H), 7.37 (dt, J = 8.6, 4.4 Hz, 4H). ^{13}C NMR (101 MHz, DMSO-d_6) δ 162.83 (d, $J_{C\text{-}F}$ = 298.2 Hz), 162.1, 160.4 (d, $J_{C\text{-}F}$ = 244.1 Hz), 159.3, 158.6, 150.8, 145.1, 142.4 (d, $J_{C\text{-}F}$ = 7.8 Hz), 135.4, 132.9 (2C), 131.98, 129.5, 129.4, 122.8, 119.8, 119.6, 118.7 (2C), 116.6, 116.3, 113.9 (d, $J_{C\text{-}F}$ = 22.8 Hz), 109.2, 102.7. HRMS (ESI) calcd for $[M+H]^+$ $C_{24}H_{16}F_2N_5O^+$: 428.1317, found: 428.1310. HPLC analysis: t_R = 12.8 min; peak area, 98.4%.

((4-((3-fluoro-2'-methyl-[1,1'-biphenyl]-4-yl)(hydroxyimino)methyl)pyrimidin-2-yl)amino) benzonitrile (7e).

Yield: 91 mg, 43%, white solid, mp: 208.6-210.2°C. ^{1}H NMR (400 MHz, DMSO- d_6) δ 12.56 (s, 1H), 10.21 (s, 1H), 8.63 (d, J = 5.2 Hz, 1H), 7.66 (d, J = 8.5 Hz, 2H), 7.50 - 7.32 (m, 10H), 2.33 (s, 3H). ^{13}C NMR (101 MHz, DMSO-d_6) δ 162.2, 159.6, 159.3, 159.1 (d, $J_{C\text{-}F}$ = 244.6 Hz) 150.8, 145.1, 144.4 (d, $J_{C\text{-}F}$ = 47.8 Hz) 140.1, 135.3, 133.0 (2C), 131.2, 131.1, 130.0, 128.4, 126.6, 125.4, 119.8, 119.2 (d , $J_{C\text{-}F}$ = 17.3 Hz), 118.7 (2C), 116.4 (d, $J_{C\text{-}F}$ = 21.9 Hz), 109.3, 102.7, 20.6. HRMS (ESI) calcd for $[M+H]^+$ $C_{25}H_{19}FN_5O^+$: 424.1568, found: 424.1575. HPLC analysis: t_R = 13.9 min; peak area, 98.8%.

((4-((3-fluoro-3'-methyl-[1,1'-biphenyl]-4-yl)(hydroxyimino)methyl)pyrimidin-2-yl)amino) benzonitrile (7f).

Yi [illegible] H),

10.21 (s, 1H), 8.63 (d, J = 5.2 Hz, 1H), 7.64 (ddd, J = 16.9, 13.1, 5.6 Hz, 7H), 7.50 - 7.47 (m, 1H), 7.43 (t, J = 8.0 Hz, 2H), 7.37 (d, J = 8.5 Hz, 2H), 7.28 (d, J = 7.6 Hz, 1H). ^{13}C NMR (101 MHz, DMSO-d_6) δ 162.1, 159.8 (d, $J_{C\text{-}F}$ = 243.9 Hz), 159.6, 159.3, 150.9, 145.1, 143.7 (d, $J_{C\text{-}F}$ = 8 Hz), 139.0, 138.9, 132.9 (2C), 131.9, 129.5, 129.4, 128.0, 124.4, 122.9, 119.8, 119.6 (d, $J_{C\text{-}F}$ = 17.9 Hz), 118.6 (2C), 114.0 (d, $J_{C\text{-}F}$ = 22.3 Hz), 109.1, 102.7, 21.6. HRMS (ESI) calcd for $[M+H]^+$ $C_{25}H_{19}FN_5O^+$: 424.1568, found: 424.1565. HPLC analysis: t_R = 14.4 min; peak area, 99.0%.

((4-((3-fluoro-4'-methyl-[1,1'-biphenyl]-4-yl)(hydroxyimino)methyl)pyrimidin-2-yl)amino) benzonitrile (7g).

Yield: 95 mg, 45%, white solid, mp: 218.1-220.3°C. ^{1}H NMR (400 MHz, DMSO-d_6) δ 12.52 (s, 1H), 10.16 (s, 1H), 8.60 (d, J = 5.2 Hz, 1H), 7.69 (d, J = 8.1 Hz, 2H), 7.66 - 7.58 (m, 4H), 7.47 - 7.39 (m, 2H), 7.34 (dd, J = 10.7, 8.2 Hz, 4H), 2.37 (s, 3H). ^{13}C NMR (101 MHz, DMSO-d_6) δ 162.2, 159.6 (d, $J_{C\text{-}F}$ = 244.1 Hz), 159.2, 158.7, 150.8, 145.2, 143.4 (d, $J_{C\text{-}F}$ = 7.8 Hz), 138.3, 136.1, 132.9 (2C), 131.9, 130.2 (2C), 127.1 (2C), 122.5, 119.8, 119.4, 118.7 (2C), 113.6 (d, $J_{C\text{-}F}$ = 22.5 Hz), 109.2, 102.7, 21.2. HRMS (ESI) calcd for $[M+H]^+$ $C_{25}H_{19}FN_5O^+$: 424.1568, found: 424.1566. HPLC analysis: t_R = 14.1 min; peak area, 99.1%.

((4-((3-fluoro-2'-methoxy-[1,1'-biphenyl]-4-yl)(hydroxyimino)methyl)pyrimidin-2-yl)amino) benzonitrile (7h).

Yield: 103 mg, 47%, white solid, mp: 183-185.7°C. ^{1}H NMR (400 MHz, DMSO-d_6) δ 12.56 (s, 1H), 10.24 (s, 1H), 8.63 (d, J = 5.1 Hz, 1H), 7.63 (d, J = 8.5 Hz, 2H), 7.52 - 7.47 (m, 3H), 7.46 - 7.37 (m, 5H), 7.23 (d, J = 8.3 Hz, 1H), 7.11 (t, J = 7.4 Hz, 1H), 3.88 (s, 3H). ^{13}C NMR (101 MHz, DMSO-d_6) δ 162.2 (d, $J_{C\text{-}F}$ = 195.3 Hz), 159.6, 159.3, 157.88, 156.5, 151.0, 145.2, 141.3 (d, $J_{C\text{-}F}$ = 8.2 Hz), 133.0 (2C), 131.0, 130.2, 130.1, 128.4, 125.5, 121.4, 119.9, 119.2 (d, $J_{C\text{-}F}$ = 17.7 Hz), 118.6 (2C), 116.5 (d, $J_{C\text{-}F}$ =

440.1518. HPLC analysis: t_R = 13.2 min; peak area, 97.5%.

((4-((3-fluoro-3'-methoxy-[1,1'-biphenyl]-4-yl)(hydroxyimino)methyl)pyrimidin-2-yl)amino) benzonitrile (7i).

Yield: 86 mg, 39%, white solid, mp: 201.5-202.7°C. ^{1}H NMR (400 MHz, DMSO-d_6) δ 12.54 (s, 1H), 10.17 (s, 1H), 8.60 (d, J = 5.2 Hz, 1H), 7.73 - 7.63 (m, 2H), 7.61 (d, J = 8.5 Hz, 2H), 7.49-7.39 (m, 3H), 7.39-7.29 (m, 4H), 7.01 (dd, J = 8.3, 2.4 Hz, 1H).3.86(s, 3H). ^{13}C NMR (101 MHz, DMSO-d_6) δ 162.1, 160.4, 159.8 (d, J_{C-F} = 246.8 Hz), 159.6, 159.3, 150.8, 145.2, 143.4 (d, J_{C-F} = 7.8 Hz), 140.5, 132.9 (2C), 131.9, 130.7, 123.0, 119.8, 119.7, 119.6, 118.7 (2C), 114.7, 114.1 (d, J_{C-F} = 22.6 Hz), 112.5, 109.1, 102.7, 55.7. HRMS (ESI) calcd for $[M+H]^+$ $C_{25}H_{19}FN_5O_2^+$: 440.1517, found: 440.1519. HPLC analysis: t_R = 13.3 min; peak area, 98.6%.

((4-((3-fluoro-4'-methoxy-[1,1'-biphenyl]-4-yl)(hydroxyimino)methyl)pyrimidin-2-yl)amino) benzonitrile (7j).

Yield: 88 mg, 40%, white solid, mp: 207.9-209.0°C. ^{1}H NMR (400 MHz, DMSO-d_6) δ 12.52 (s, 1H), 10.17 (s, 1H), 8.60 (d, J = 5.2 Hz, 1H), 7.75 (d, J = 8.7 Hz, 2H), 7.66 - 7.57 (m, 4H), 7.47 - 7.33 (m, 4H), 7.10 - 7.04 (m, 2H), 3.81 (s, 3H). ^{13}C NMR (101 MHz, DMSO-d_6) δ 162.2, 160.0, 160.0 (d, J_{C-F} = 234.9 Hz), 159.6, 159.2, 150.9, 145.2, 143.2 (d, J_{C-F} = 8.1 Hz), 132.9 (2C), 131.9, 131.2, 128.5 (2C), 122.2, 119.8, 118.6 (2C), 115.0 (2C), 115.0, 113.3 (d, J_{C-F} = 22.1 Hz), 109.2, 102.7, 55.7. HRMS (ESI) calcd for $[M+H]^+$ $C_{25}H_{19}FN_5O_2^+$: 440.1517, found: 440.1536. HPLC analysis: t_R = 13.0 min; peak area, 97.6%.

((4-((2'-chloro-3-fluoro-[1,1'-biphenyl]-4-yl)(hydroxyimino)methyl)pyrimidin-2-yl)amino) benzonitrile (7k).

Yi [illegible] H), 9.27 (s, 1H), 8.60 (d, J = 5.2 Hz, 1H), 7.78 (d, J = 8.9 Hz, 2H), 7.65 (d, J = 7.2 Hz, 1H), 7.61-7.54 (m, 3H), 7.54 - 7.49 (m, 3H), 7.49 - 7.44 (m, 3H). ^{13}C NMR (101 MHz, Acetone-d_6) δ 161.23 (d, $J_{C\text{-}F}$ = 177.1 Hz), 159.62, 158.67, 157.89, 151.1, 144.6, 142.0 (d, $J_{C\text{-}F}$ = 8.3 Hz), 138.7, 132.7 (2C), 131.8, 131.6, 131.0 (d, J = 4.6 Hz), 130.3, 129.7, 127.6, 125.1 (d, $J_{C\text{-}F}$ = 3.1 Hz), 118.9, 118.4 (2C), 118.3, 116.4 (d, $J_{C\text{-}F}$ = 22.6 Hz), 109.0, 103.5. HRMS (ESI) calcd for $[M+H]^+$ $C_{24}H_{16}ClFN_5O^+$: 444.1022, found: 444.1015. HPLC analysis: t_R = 13.0 min; peak area, 97.6%.

((4-((4'-chloro-3-fluoro-[1,1'-biphenyl]-4-yl)(hydroxyimino)methyl)pyrimidin-2-yl)amino) benzonitrile (7l).

Yield: 93 mg, 42%, white solid, mp >250°C. ^{1}H NMR (400 MHz, DMSO-d_6) δ 12.56 (s, 1H), 10.17 (s, 1H), 8.60 (d, J = 5.2 Hz, 1H), 7.89 - 7.82 (m, 2H), 7.74 - 7.64 (m, 2H), 7.64 - 7.54 (m, 4H), 7.49-7.42 (m, 2H), 7.36 (d, J = 8.5 Hz, 2H). ^{13}C NMR (101 MHz, DMSO-d_6) δ 162.1, 159.9 (d, $J_{C\text{-}F}$ = 244.2 Hz), 159.6, 159.3, 150.7, 145.1, 142.1 (d, $J_{C\text{-}F}$ = 8.1 Hz), 137.7, 133.7, 132.9 (2C), 132.1, 129.6 (2C), 129.1 (2C), 122.8, 120.1 (d, $J_{C\text{-}F}$ = 17.8 Hz), 119.8, 118.7 (2C), 114.0 (d, $J_{C\text{-}F}$ = 22.8 Hz), 109.2, 102.7. HRMS (ESI) calcd for $[M+H]^+$ $C_{24}H_{16}ClFN_5O^+$: 444.1022, found: 444.1029. HPLC analysis: t_R = 14.0 min; peak area, 97.5%.

((4-((3-fluoro-2'-(trifluoromethyl)-[1,1'-biphenyl]-4-yl)(hydroxyl-imino)methyl)pyrimidin-2-yl) amino)benzonitrile (7m).

Yield: 83 mg, 35%, white solid, mp: 217.5-218.3°C. ^{1}H NMR (400 MHz, DMSO-d_6) δ 12.62 (s, 1H), 10.23 (s, 1H), 8.64 (d, J = 5.2 Hz, 1H), 7.92 (d, J = 7.9 Hz, 1H), 7.80 (t, J = 7.6 Hz, 1H), 7.73 - 7.65 (m, 3H), 7.47 (dd, J = 8.9, 4.8 Hz, 5H), 7.40 (d, J = 10.3 Hz, 1H), 7.33 (d, J = 7.9 Hz, 1H). ^{13}C NMR (101 MHz, DMSO-d_6) δ162.0, 159.7, 159.4, 158.8 (d, $J_{C\text{-}F}$ = 245.1 Hz), 150.5, 145.1, 142.4 (d, $J_{C\text{-}F}$ = 8.2 Hz), 139.4, 133.1 (2C), 133.0, 132.6, 131.1, 129.2, 127.3 (d, $J_{C\text{-}F}$ = 29.3 Hz), 126.8 (q, $J_{C\text{-}F}$ = 5.5 Hz), 126.0,

  for

$[M+H]^+$ $C_{25}H_{16}F_4N_5O^+$: 478.1285, found: 478.1271. HPLC analysis: t_R = 13.9 min; peak area, 99.2%.

((4-((3-fluoro-4'-(trifluoromethyl)-[1,1'-biphenyl]-4-yl)(hydroxyl-imino)methyl)pyrimidin-2-yl) amino)benzonitrile (7n).

Yield: 98 mg, 41%, white solid, mp: 210.7-211.4°C. ^{1}H NMR (400 MHz, DMSO-d_6) δ 12.62 (s, 1H), 10.20 (s, 1H), 8.63 (d, J = 5.2 Hz, 1H), 8.06 (d, J = 8.0 Hz, 2H), 7.90 (d, J = 8.1 Hz, 2H), 7.79 (ddd, J = 18.5, 9.4, 1.7 Hz, 2H), 7.64 (d, J = 8.5 Hz, 2H), 7.56 - 7.46 (m, 2H), 7.38 (d, J = 8.5 Hz, 2H). ^{13}C NMR (101 MHz, DMSO-d_6) δ162.0, 159.9 (d, J_{C-F} = 244.6 Hz), 159.6, 159.3, 150.6, 145.1, 142.9, 141.8 (d, J_{C-F} = 8.0 Hz), 133.0 (2C), 132.2, 130.1, 129.1 (d, J_{C-F} = 31.6 Hz), 128.2, 126.4 (q, J_{C-F} = 3.8 Hz), 126.1, 124.8, 123.3, 120.8 (d, J_{C-F} = 17.6 Hz), 119.8, 118.7 (2C), 114.5 (d, J_{C-F} = 22.8 Hz), 109.2, 102.72. HRMS (ESI) calcd for $[M+H]^+$ $C_{25}H_{16}F_4N_5O^+$: 478.1285, found: 478.1268. HPLC analysis: t_R = 13.3 min; peak area, 99.7%.

Biological assays

In vitro anti-HIV assay

Evaluation of the antiviral activity of the compounds against WT HIV-1, and mutant strains (L100I, K103N, E138K, Y188L and Y181C) in MT-4 cells was performed using the MTT assay [21]. Stock solutions (10 x final concentration) of test compounds were added in 25 μL volumes to two series of triplicate wells so as to allow simultaneous evaluation of their effects on mock- and HIV-infected cells at the beginning of each experiment. Serial 5-fold dilutions of test compounds were made directly in flat-bottomed 96-well microtiter trays using a Biomek 3000 robot (Beckman instruments, Fullerton, CA). Untreated HIV- and mock-infected cell samples were included as controls. HIV stock (50 μL) at 100-300 CCID50 (50% cell culture infectious doses) or culture medium was added to either the infected or mock-infected wells of the microtiter tray. Mock-infected cells were used to evaluate the effects of test

growing MT-4 cells were centrifuged for 5 minutes at 220 g and the supernatant was discarded. The MT-4 cells were resuspended at 6 x 10^5 cells/mL and 50 µL volumes were transferred to the microtiter tray wells. Five days after infection, the viability of mock-and HIV-infected cells was examined spectrophotometrically using the MTT assay. The MTT assay is based on the reduction of yellow colored 3-(4,5-dimethylthiazol-2-yl)-2,5-diphenyltetrazolium bromide (MTT) (Acros Organics) by mitochondrial dehydrogenase activity in metabolically active cells to a blue-purple formazan that can be measured spectrophotometrically. The absorbances were read in an eight-channel computer-controlled photometer (Infinite M1000, Tecan), at two wavelengths (540 and 690 nm). All data were calculated using the median absorbance value of three wells. The 50% cytotoxic concentration (CC_{50}) was defined as the concentration of the test compound that reduced the absorbance (OD540) of the mock-infected control sample by 50%. The concentration achieving 50% protection against the cytopathic effect of the virus in infected cells was defined as the 50% effective concentration (EC_{50}).

Reverse transcriptase assay

Recombinant wild type p66/p51 HIV-1 RT was expressed and purified as previously described [22]. The RT assay is performed with the EnzCheck Reverse Transcriptase Assay kit (Molecular Probes, Invitrogen), as described by the manufacturer. The assay is based on the dsDNA quantitation reagent PicoGreen. This reagent shows a pronounced increase in fluorescence signal upon binding to dsDNA or RNA-DNA heteroduplexes. Single-stranded nucleic acids generate only minor fluorescence signal enhancement when a sufficiently high dye: base pair ratio is applied [23]. This condition is met in the assay. A poly(rA) template of approximately 350 bases long, and an oligo (dT)16 primer, are annealed in a molar ratio of 1: 1.2 (60 min. at room temperature). Fifty-two ng of the RNA/DNA is brought into each well of a 96-well plate in a volume of 20 µL polymerization buffer (60 mM Tris-HCl, 60 mM KCl, 8 mM $MgCl_2$, 13 mM DTT, 100 µM dTTP, pH 8.1). 5 µL of RT enzyme solution, diluted to a suitable

The reactions are incubated at 25°C for 40 minutes and then stopped by the addition of EDTA (15 mM). Heteroduplexes are then detected by addition of PicoGreen. Signals are read using an excitation wavelength of 490 nm and emission detection at 523 nm using a spectrofluorometer (Safire 2, Tecan). To test the activity of compounds against RT, 1 µL of compound in DMSO is added to each well before the addition of RT enzyme solution. Control wells without compound contain the same amount of DMSO. Results are expressed as relative fluorescence. The fluorescence signal of the reaction mix with compound divided by the signal of the same reaction mix without compound.

Molecular modelling

The modelling study was carried out by Schrödinger Maestro 11.4 [24]. The first step was the protein, HIV-1 RT (PDB entry: 2ZD1) preparation, which followed a standard protocol. Before the preparation, the protein was prepared by removing water molecules, the ligand, and other unnecessary molecules from the crystal structure of the HIV-1 RT complex. After that the docking study was performed using Glide. The parameters choose the default without any constraints. Final scoring was then obtained on the energy-minimized poses. MD simulations were carried out for RT in complex with the compound scoring lowest one. Each system was solvated in a cubic box with explicit TIP3P water and counter ions consisting of a 10 Å solvent buffer region from the edge of the complex. The long range electrostatic interactions were evaluated by the Particle-Mesh Ewald method under the periodic boundary condition. 3 ns simulation was carried out for each docked model using Desmond with OPLS-AA 2005 force field. The stability of the simulation was assessed by monitoring the RMSD with respect to the minimized starting structure. The molecular docking result was generated using PyMol (http://pymol.sourceforge.net/) [6-8, 25, 26].

Acknowledgements

W by the China Association for Science and Technology (2017QNRC061). The technical assistance of Kristien Erven, Cindy Heens and of Kris Uyttersprot for the HIV experiments and HIV RT polymerase assays is gratefully acknowledged.

References

[1] WHO website. HIV/AIDS fact sheet, 15 November,2019. https://www.who.int/en/news-room/fact-sheets/detail/hiv-aids.
[2] H. Liu, Y. Ma, Y. Su, M.K. Smith, Y. Liu, Y. Jin, H. Gu, J. Wu, L. Zhu, N. Wang, Emerging trends of HIV drug resistance in Chinese HIV-infected patients receiving first-line highly active antiretroviral therapy: a systematic review and meta-analysis, Clin. Infect. Dis. 59 (2014) 1495-502.
[3] D. Li, P. Zhan, E. De Clercq, X. Liu, Strategies for the Design of HIV-1 Non-Nucleoside Reverse Transcriptase Inhibitors: Lessons from the Development of Seven Representative Paradigms, J. Med. Chem. 55 (2012) 3595-3613.
[4] Y. Mehellou, E. De Clercq, Twenty-Six Years of Anti-HIV Drug Discovery: Where Do We Stand and Where Do We Go?, J. Med. Chem. 53 (2010) 521-538.
[5] K. Jin, H. Yin, E. De Clercq, C. Pannecouque, G. Meng, F. Chen, Discovery of biphenyl-substituted diarylpyrimidines as non-nucleoside reverse transcriptase inhibitors with high potency against wild-type and mutant HIV-1, Eur. J. Med. Chem. 145 (2018) 726-734.
[6] Y. Sang, S. Han, C. Pannecouque, E. De Clercq, C. Zhuang, F. Chen, Conformational restriction design of thiophene-biphenyl-DAPY HIV-1 non-nucleoside reverse transcriptase inhibitors, Eur. J. Med. Chem. 182 (2019) 111603.
[7] Y. Sang, S. Han, C. Pannecouque, E. De Clercq, C. Zhuang, F. Chen, Ligand-Based Design of Nondimethylphenyl-Diarylpyrimidines with Improved Metabolic Stability, Safety, and Oral Pharmacokinetic Profiles, J. Med. Chem. 62 (2019) 11430-11436.
[8] K. Jin, M. Liu, C. Zhuang, E. De Clercq, C. Pannecouque, G. Meng, F. Chen, Improving the positional adaptability: structure-based design of biphenyl-substituted diaryltriazines as novel non-nucleoside HIV-1 reverse transcriptase inhibitors, Acta Pharm. Sin. B 10 (2020) 344-357.
[9] C. Zhuang, C. Pannecouque, E. De Clercq, F. Chen, Development of non-nucleoside reverse transcriptase inhibitors (NNRTIs): Our past twenty years, Acta Pharm. Sin. B (2019), doi: 10.1016/j.apsb.2019.11.010.
[10] M. Katalinić, G. Šinko, N. Maček Hrvat, T. Zorbaz, A. Bosak, Z. Kovarik, Oxime-assisted reactivation of tabun-inhibited acetylcholinesterase analysed by active site mutations, Toxicology 406-407 (2018) 104-113.
[11] D.L. Hughes, Patent Review of Manufacturing Routes to Fifth-Generation Cephalosporin Drugs. Part 2, Ceftaroline Fosamil and Ceftobiprole Medocaril, Org. Process Res. Dev. 21 (2017) 800-815.
[12] O.B. Flekhter, E.I. Boreko, L.R. Nigmatullina, N.I. Pavlova, N.I. Medvedeva, S.N. Nikolaeva, E.V. Tret'yakova, O.V. Savinova, L.A. Baltina, L.T. Karachurina, F.Z. Galin, F.S. Zarudii, G.A. Tolstikov, Synthesis and Pharmacological Activity of Acylated Betulonic Acid Oxides and 28-Oxo-Allobetulone, Pharm. Chem. J. 38 (2004) 148-152.
[13] C. M. Ma, N. Nakamura, M. Hattori, T. Kawahata, T. Otake, Inhibitory effects of triterpene-azidothymidine conjugates on proliferation of human immunodeficiency virus type 1 and its protease, Chem. Pharm. Bull. 50 (2002) 877-880.
[14] L.-L. Wang, N. Battini, R. R. Y. Bheemanaboina, M. F. Ansari, J.-P. Chen, Y.-P. Xie, G.-X. Cai, S.-

L. [illegible] ti-targeting antibacterial agents: Design, synthesis and evaluation acting on microbes, DNA, HSA and topoisomerase IV, Eur. J. Med. Chem. 179 (2019) 166-181.
[15] B. Bednarczyk-Cwynar, L. Zaprutko, Recent advances in synthesis and biological activity of triterpenic acylated oximes, Phytochem. Rev. 14 (2015) 203-231.
[16] V. P. Mehta, A. Sharma, S. G. Modha, S. Sharma, T. Meganathan, V. S. Parmar, E. Van der Eycken, N-heterocyclic carbene catalyzed aroylation of 3,5-dichloro-2(1H)-pyrazinones, J. Org. Chem. 76 (2011) 2920-5.
[17] Y. Suzuki, N. Iwata, K. Dobashi, R. Takashima, S. Arulmozhiraja, E. Ishitsubo, N. Matsuo, H. Tokiwa, Alkanoylation of quinazoline by nucleophilic aromatic substitution: Combined experimental and computational study, Tetrahedron 74 (2018) 392-400.
[18] B. Chakravarti, T. Akhtar, B. Rai, M. Yadav, J. Akhtar Siddiqui, S.K. Dhar Dwivedi, R. Thakur, A.K. Singh, A.K. Singh, H. Kumar, K. Khan, S. Pal, S.K. Rath, J. Lal, R. Konwar, A.K. Trivedi, D. Datta, D.P. Mishra, M.M. Godbole, S. Sanyal, N. Chattopadhyay, A. Kumar, Thioaryl naphthylmethanone oxime ether analogs as novel anticancer agents, J. Med. Chem. 57 (2014) 8010-8025.
[19] M.L. Liu, X.Y. Pan, T. Yang, W.M. Zhang, T.Q. Wang, H.Y. Wang, H.X. Lin, C.G. Yang, Y.M. Cui, The synthesis and antistaphylococcal activity of dehydroabietic acid derivatives: Modifications at C-12, Bioorg. Med. Chem. Lett. 26 (2016) 5492-5496.
[20] Y. Sang, S. Han, C. Pannecouque, E. De Clercq, C. Zhuang, F. Chen, Ligand-Based Design of Nondimethylphenyl-Diarylpyrimidines with Improved Metabolic Stability, Safety, and Oral Pharmacokinetic Profiles, J. Med. Chem. 62 (2019) 11430-11436.
[21] E.P. Gillis, K.J. Eastman, M.D. Hill, D.J. Donnelly, N.A. Meanwell, Applications of Fluorine in Medicinal Chemistry, J. Med. Chem. 58 (2015) 8315-8359.
[22] C. Pannecouque, D. Daelemans, E. De Clercq, Tetrazolium-based colorimetric assay for the detection of HIV replication inhibitors: revisited 20 years later, Nat. Protoc. 3 (2008) 427-434.
[23] J. Auwerx, T.W. North, B.D. Preston, G.J. Klarmann, E. De Clercq, J. Balzarini, Chimeric human immunodeficiency virus type 1 and feline immunodeficiency virus reverse transcriptases: Role of the subunits in resistance/sensitivity to non-nucleoside reverse transcriptase inhibitors, Mol. Pharmacol. 61 (2002) 400-406.
[24] C. Zhuang, S. Narayanapillai, W. Zhang, Y.Y. Sham, C. Xing, Rapid Identification of Keap1–Nrf2 Small-Molecule Inhibitors through Structure-Based Virtual Screening and Hit-Based Substructure Search, J. Med. Chem. 57 (2014) 1121-1126.
[25] S. Han, Y. Sang, Y. Wu, Y. Tao, C. Pannecouque, E. De Clercq, C. Zhuang, F.E. Chen, Molecular Hybridization-Inspired Optimization of Diarylbenzopyrimidines as HIV-1 Nonnucleoside Reverse Transcriptase Inhibitors with Improved Activity against K103N and E138K Mutants and Pharmacokinetic Profiles, ACS Infect. Dis. (2019), doi:10.1021/acsinfecdis.9b00229.
[26] S. Han, Y. Lei, C. Pannecouque, E. De Clercq, C. Zhuang, F. Chen, Fragment-based discovery of sulfur-containing diarylbenzopyrimidines as novel nonnucleoside reverse transcriptase inhibitors, Chin. Chem. Lett. 31 (2020) 764-768.

Graphic Abstract

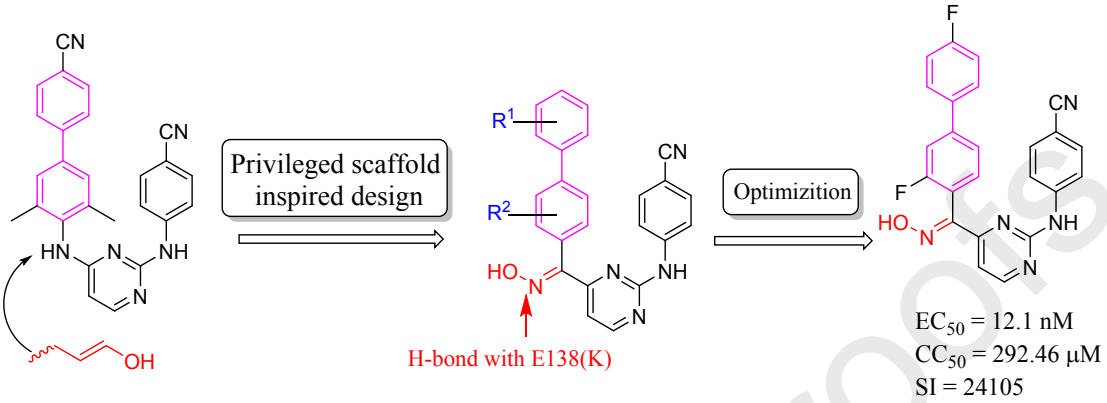

Novel oxime-biphenyl-DAPYs were designed and synthesized by a privileged scaffold inspired strategy, exhibiting promising anti-HIV activity, low cytotoxicity and high selectivity index.

1. Fourteen oxime-biphenyl-DAPYs were designed by a privileged scaffold inspired strategy.
2. These compounds possessed up to nanomolar potency and low toxicity against wild-type HIV-1-infected cells.
3. Compound **7d** displayed a high potency against WT (EC_{50} = 12.1 nM), E138K mutant strains (EC_{50} = 0.027 μM) and a high selective index (SI = 24105).

☒ The authors declare that they have no known competing financial interests or personal relationships that could have appeared to influence the work reported in this paper.

☐The authors declare the following financial interests/personal relationships which may be considered as potential competing interests: